

Title: Lipid nanoparticles and siRNA targeting plasminogen provide lasting inhibition of fibrinolysis in mouse and dog models of hemophilia A

Authors: Amy W Strilchuk^{1,2}, Woosuk S Hur³, Paul Batty⁴, Yaqiu Sang³, Sara R Abrahams³, Alyssa SM Yong¹, Jerry Leung^{1,2}, Lakmali M Silva⁵, Jocelyn A Schroeder^{6,7}, Kate Nesbitt⁴, Bas de Laat⁸, Niki M Moutsopoulos⁵, Thomas H Bugge⁵, Qizhen Shi^{6,7}, Pieter R Cullis², Elizabeth P Merricks³, Alisa S Wolberg³, Matthew J Flick³, David Lillicrap⁴, Timothy C Nichols³, Christian J Kastrup^{1,2,6,9}

Affiliations:

¹ Michael Smith Laboratories, University of British Columbia, Vancouver, V6T 1Z4, Canada.

² Department of Biochemistry and Molecular Biology, University of British Columbia, Vancouver, V6T 2A1, Canada.

³ Department of Pathology and Laboratory Medicine and UNC Blood Research Center, University of North Carolina at Chapel Hill, Chapel Hill, NC, 27599, USA.

⁴ Department of Pathology and Molecular Medicine, Queen's University, Kingston, ON, K7L 3N6, Canada.

⁵ National Institute of Dental and Craniofacial Research, National Institutes of Health, Bethesda, MD, 20892, USA.

⁶ Blood Research Institute, Versiti, Milwaukee, WI, 53226, USA.

⁷ Department of Pediatrics, Medical College of Wisconsin, Milwaukee, WI, 53226, USA.

⁸ Synapse Research Institute, Maastricht, 6217 KM, Netherlands.

⁹ Departments of Surgery, Biochemistry, Biomedical Engineering, and Pharmacology and Toxicology, Medical College of Wisconsin, Milwaukee, WI, 53226, USA.

Corresponding author: Dr. Christian J Kastrup email: ckastrup@versiti.org.

OVERLINE: BLOOD DISORDERS

Once Sentence Summary: Plasminogen knockdown, achieved using siRNA contained in lipid nanoparticles, improves hemostasis in murine and canine models of hemophilia

A.

Editor's summary:

Abstract: Antifibrinolytic drugs are used extensively for on-demand treatment of severe acute bleeding. Controlling fibrinolysis may also be an effective strategy to prevent or lessen chronic recurring bleeding in bleeding disorders such as hemophilia A (HA), but current antifibrinolytics have unfavorable pharmacokinetic profiles. Here we developed a long-lasting antifibrinolytic using small interfering RNA (siRNA) targeting plasminogen and packaged in clinically-used lipid nanoparticles (LNPs) and tested it to determine if reducing plasmin activity in animal models of HA could decrease bleeding frequency and severity. Treatment with the siRNA-carrying LNPs reduced circulating plasminogen and suppressed fibrinolysis in wild-type and HA mice and dogs. In HA mice, hemostatic efficacy depended on the injury model; plasminogen knockdown improved hemostasis after a saphenous vein injury, but not tail vein transection injury, suggesting that saphenous vein injury is a murine bleeding model sensitive to the contribution of fibrinolysis. In dogs with HA, LNPs carrying siRNA targeting plasminogen were as effective at stabilizing clots as tranexamic acid, a clinical antifibrinolytic, and in a pilot study of two dogs with HA, the incidence of spontaneous or excess bleeding was reduced during four months of prolonged knockdown. Collectively, these data demonstrate that long-acting antifibrinolytic therapy can be achieved and that it provides hemostatic benefit in animal models of HA.

INTRODUCTION

Fibrinolysis is a proteolytic process that remodels and clears blood clots from the vasculature. The enzymes of the fibrinolytic pathway become activated both during and after clot formation, opposing the growth of the fibrin clot and ultimately restoring blood flow through vessels (1). The generation of plasmin, the protease that cleaves fibrin, from its proenzyme plasminogen, is mediated by tissue plasminogen activator (tPA) and urokinase (uPA) (2). Plasmin generation is suppressed by endogenous antifibrinolytics, such as plasminogen activator inhibitor-1 (PAI-1), and is pharmacologically inhibited by the small-molecules tranexamic acid (TXA) and ϵ -aminocaproic acid (EACA) (3). Fibrinolysis is also regulated by thrombin generation; thrombin converts fibrinogen to fibrin which acts as a cofactor for tPA-mediated plasminogen activation. Thrombin also activates thrombin-activated fibrinolysis inhibitor (TAFI) and coagulation factor XIII, which modify fibrin to decrease the rate of lysis (3).

Fibrin formation and degradation must be balanced to maintain hemostasis. When coagulation is compromised, fibrinolysis can further impede hemostasis (1). For example, hemophilia A (HA) is caused by a deficiency in coagulation factor VIII (FVIII) and results in low thrombin generation after vascular injury. This in turn leads to clots with abnormal fibrin structure that are more susceptible to lysis, as well as more active fibrinolysis (4–6). Patients with HA suffer from spontaneous bleeding in joints and mucosal tissue and excessive bleeding after injury, caused by a combination of less thrombin activity and higher plasmin activity (7). Patients with bleeding disorders greatly benefit from prophylactic therapeutic regimens to prevent bleeding episodes (8), however the use of current antifibrinolytics, such as TXA, is limited to on-demand treatment after bleeding has commenced since their circulating half-lives are 3 hours or less (9).

Gene silencing, such as with small interfering RNA (siRNA), has been used in mice to achieve long-lasting control of proteins involved in hemostasis, including fibrinogen (10), coagulation factor XI (11), XII (12), and XIII (13) and a disintegrin and metalloproteinase with a thrombospondin type 1 motif, member 13 (ADAMTS13) (14), and used in clinical trials for bleeding disorders by knocking down antithrombin (15). Lipid nanoparticles (LNPs) can effectively deliver siRNA to hepatocytes, where plasminogen is synthesized, and have been used in three clinically-approved RNA-based therapies (16–18). In this study, we tested the hypothesis that siRNA knockdown of plasminogen can achieve long-lasting suppression of fibrinolysis and can be used as a prophylactic therapy to maintain hemostasis in HA. This work adds to previous studies probing the impact of fibrinolysis in murine hemostasis (2, 19), and tests the efficacy of siRNA

delivered with LNPs in canine HA, which is a large animal model of human bleeding disorders (20).

RESULTS

siRNA delivered via LNP depletes circulating plasminogen for weeks after a single administration

siRNA was designed to specifically knock-down plasminogen (siPlg) in mice or dogs. siPlg encapsulated in ionizable cationic lipid nanoparticles was administered to all mice at a dose of 1 mg siRNA per kg body weight (mg/kg). Three days after the first administration to wild-type C57BL/6 mice, *Plg* mRNA was knocked down by $95\pm 0.67\%$, and plasminogen protein was correspondingly depleted from plasma, compared to control mice treated with siRNA targeting luciferase (siLuc) (Fig. 1, A and B). Wild-type mice administered a single dose of siPlg exhibited plasminogen knockdown for over four weeks, while those that received siLuc exhibited only standard variation of baseline plasminogen expression (15, 16) (Fig. 1C). In healthy wild-type dogs of hound background, the extent and duration of plasminogen knockdown was dependent on the dose of siRNA-LNPs (Fig. 1D). A single dose of 0.54 mg/kg in one dog resulted in over six weeks of plasminogen knockdown. A ten-fold lower dose in the same and an additional dog, 0.054 mg/kg, depleted 75-85% of plasminogen protein from plasma for four weeks, while 0.027 mg/kg achieved only modest depression of protein expression in the same two dogs and another (Fig. 1, D and E). No changes in the behavior or appetite of the dogs treated with LNPs were observed. However, the 0.54 mg/kg dose increased liver enzymes transiently over 10 days, which was reduced at lower doses, and was independent of plasminogen knockdown (fig. S1, A and B). Alanine transaminase (ALT) and aspartate transaminase (AST) were most elevated after first exposure to LNPs and waned with subsequent doses (fig. S1, C and D); c-reactive protein was below 5 mg/L at every measurement.

Prolonged siRNA-mediated plasminogen knockdown in mice does not induce phenotypes associated with complete plasminogen deficiency

Repeated siRNA administration to healthy C57BL/6 mice at three-week intervals maintained circulating plasminogen below 25% of baseline for nine months. Whereas mice with genetic plasminogen knockout (*Plg*^{-/-}) are prone to wasting disease, leading to weight loss over time (23), prolonged siPlg treatment did not impact mouse weight compared to siLuc treatment (Fig. 2A). *Plg*^{-/-} mice also demonstrate gastrointestinal and mucosal immunopathology, including periodontitis, and fibrin deposition, resulting in spontaneous extravascular fibrin-rich lesions (liver,

stomach, and lung) at 5-12 weeks of age (24, 25). In this study, histopathological assessments after nine months of siRNA-mediated plasminogen depletion demonstrated no signs of periodontal bone loss (Fig. 2B), nor the processes that contribute to immunopathology in plasminogen deficiency, such as interleukin-mediated inflammation (Fig. 2, C to F). There were no elevations in hepatic expression of interleukin 6 (*Il6*), or systemic tumour necrosis factor alpha ($\text{TNF}\alpha$) or IL-6 protein, however hepatic expression of *Tnf* was elevated in both siLuc and siPIg-treated mice compared to untreated age-matched controls (Fig. 2, C to F). Mice exhibited mild elevations of interleukins (IL-6, IL-5, IL-10, and IL-1 β), proinflammatory markers $\text{TNF}\alpha$, and keratinocyte chemoattractant (KC)/growth-regulated oncogenes (GRO), and liver enzymes ALT and AST immediately after their first exposure to siRNA-LNPs, but none of these were elevated after nine months of repeated dosing (fig. S2).

After nine months of plasminogen knockdown, there were no signs of fibrin deposition in the liver of treated mice (Fig. 2G, fig. S3, A and B); and in a separate cohort of mice administered siPIg bi-weekly for 5 months, there were no obvious differences in lung morphology or evidence of fibrin deposition in the lung (fig. S3, C and D). In whole blood clots formed *ex vivo*, there were no obvious differences in fibrin structure between siLuc and siPIg treatment groups (Fig. 2H).

Plasminogen knockdown promotes hemostasis in HA mice after saphenous vein puncture, but not tail vein transection

The potential hemostatic benefits of antifibrinolysis in different types of bleeds in HA were evaluated in different models of induced bleeding in *FVIII*^{-/-} mice (Fig. 3A). HA mice were treated with 1 mg/kg siPIg two weeks prior to the injury, resulting in 96% plasminogen protein depletion compared to untreated *FVIII*^{-/-} mice (Fig. 3B). After tail-vein-transection (TVT), siPIg-treated HA mice exhibited no difference in blood loss compared to untreated HA mice; both treated and untreated HA groups lost significantly more blood than WT controls ($P = 0.013$ and $P = 0.0061$, respectively) (Fig. 3C). Mean bleed time after TVT in siPIg-treated HA mice was 26.0 ± 8.6 minutes, compared to 41.8 ± 3.7 minutes in untreated HA mice, and 3.3 ± 0.5 minutes in WT controls, but the difference between untreated HA mice and siPIg-treated HA mice was non-significant (Fig. 3D). In contrast, in a saphenous-vein-puncture (SVP) model, both blood loss and bleeding time were reduced in HA mice treated with siPIg two-weeks prior to injury, similar to wild-type controls (Fig. 3, E and F).

siRNA targeting plasminogen reduces bleeding events in HA dogs and stabilizes clots similar to clinical antifibrinolytics

In HA dogs with FVIII deficiency, clot stability was measured using thromboelastography in plasma samples collected at baseline, 4 hours after administration of TXA (10 mg/kg IV), and/or one week after siPIg administration (0.054 mg/kg IV). Plasma clot lysis with exogenous tPA was delayed in samples collected within 4 hours of TXA administration, or one week after siPIg administration, compared to baseline samples (Fig. 4, A and B). Clot stability was not additionally enhanced when TXA was administered to dogs already treated with siPIg (Fig. 4, A and B). Other clot parameters, such as clot strength (maximum amplitude) and clotting time (alpha angle and R-time), were not changed, and prothrombin time, fibrinogen concentration, antithrombin activity, and D-dimer concentrations all remained within or close to normal range in the HA dogs (fig. S4). Thrombin and plasmin generation were reduced in plasma from HA dogs compared to wild-type dogs (Fig. 4, C to F). In plasma samples collected from siPIg-treated animals, residual plasminogen concentration did not significantly correlate with peak thrombin generation ($P = 0.246$) (Fig. 4D), but did significantly correlate with peak plasmin generation ($P = 0.001$) (Fig. 4F).

The canine hemophilia A model demonstrates similarities in bleeding phenotype and treatment to human HA (20). To assess the prophylactic potential of siPIg, two HA dogs were administered 0.054 mg/kg siPIg every three weeks for 15 weeks. Plasma plasminogen was maintained at <50% of baseline values (Fig. 5A). Annualized bleeding rates were reduced on siPIg treatment compared to a ten month observation period before initiation of siPIg, when bleed rates were similar to what has been previously reported (26) (Fig. 5B). Whereas in the ten months prior to treatment one dog had experienced five hematomas or joint bleeds and the other dog experienced one, neither dog experienced a joint bleed or hematoma during the siPIg treatment period. During the four months of treatment with siPIg, one dog experienced two instances of mouth bleeds and one instance of excess bleeding from an IV puncture site. No clinical evidence of overt thromboembolic disease was observed during siPIg treatment.

DISCUSSION

Antifibrinolytics such as TXA and EACA are used to reduce bleeding in diverse clinical scenarios including: postpartum hemorrhage, pre-hospital trauma, surgical hemorrhage, and bleeding disorders (27–33). Mortality in trauma and post-partum hemorrhage may be reduced by TXA, but only if administered within hours of the onset of bleeding (34, 35); this suggests that fibrinolysis contributes early in bleeding, and a prophylactic antifibrinolytic approach may be beneficial for preventing major bleeding episodes as well as restoring hemostasis. However, the short half-life of current antifibrinolytics preclude their usage for prophylaxis. Here we evaluated siRNA-LNPs

as a strategy to inhibit hepatic plasminogen expression. This resulted in sustained plasma plasminogen depletion and reduced fibrinolytic activity. siRNA-LNPs achieved a dose-dependent knockdown of plasminogen, consistent with previous studies knocking down other hepatic proteins (36–38). In mice and dogs, at doses of 1 mg/kg and 0.054 mg/kg, respectively, siPlg caused plasminogen protein depletion of >75% for multiple weeks after a single administration, and knockdown could be sustained for months by repeat administration at three-week intervals.

Dogs with FVIII deficiency are a translationally relevant model with the types, size and duration of bleeds similar to humans with hemophilia A. In dogs with HA, siPlg stabilized clots equally to therapeutic TXA, a commonly used antifibrinolytic in dogs. Consistent with previous studies, plasminogen knockdown did not impact thrombin peak (39, 40), though TXA did appear to reduce thrombin generation through an unknown mechanism. During a 4-month period of sustained plasminogen knockdown, the number of bleeding events experienced by two HA dogs was reduced, compared to pre-treatment. The role of fibrinolysis in hemostasis appears to be weaker in mice compared to in humans or canines. For example, previous studies showed that mice deficient in PAI-1 or α 2-plasmin inhibitor do not exhibit overt bleeding, despite these deficiencies being associated with spontaneous bleeding in humans (2). Previous studies also showed no hemostatic benefit after a tail-vein transection model of injury in mice with combined plasminogen and FVIII genetic knockout (19, 41). While we did not directly compare bleeding between mice with complete plasminogen knockout versus knockdown, we confirmed that this result held true with siRNA knockdown of plasminogen. However, in a different injury model, the saphenous vein puncture, plasminogen knockdown reduced blood loss and bleeding time. We hypothesize this difference is due to the type of injury, which may be more sensitive to changes in clot fibrinolysis. Saphenous vein injury models are less severe, less dependent on the action of platelets, and exhibit greater sensitivity to factors seen in hemophilia conditions, such as low plasma FVIII concentrations (42, 43). Further differences may include the amount of tissue damage, the blood flow shear rate, the inflammation resulting from the injury models, and the availability of tissue matrix to hold unstable clots at the site of injury, although these require further detailed study.

Although plasminogen deficiency is not associated with an elevated risk of thrombosis (44–48), both humans and mice exhibit other adverse effects, including liginous conjunctivitis, periodontal bone loss, and fibrin deposition in various tissues (25, 49–52). Liginous conjunctivitis has also been induced by continuous TXA administration, which is reversed on stopping TXA treatment (53). If these symptoms were to occur with siPlg, they might be reversed by a combination of stopping treatment and replacing plasminogen with transfusion of plasma or purified protein, or

plasminogen-containing eyedrops, as is done in cases of plasminogen deficiency. The absence of adverse phenotypes associated with plasminogen deficiency after prolonged plasminogen knockdown by siPlg was likely due to the low residual plasminogen expression. This is supported by the fact that heterozygous *Plg*^{+/-} mice do not display the spontaneous pathologies seen in plasminogen knockout mice (24, 25). This study suggests that less than 25% of baseline plasminogen is required to avoid these pathologies. By achieving substantial plasminogen knockdown for weeks after a single administration, while avoiding the *Plg*⁻-associated disease state, siPlg may enable long-term studies of antifibrinolytic therapy in disease models where plasminogen has been implicated as a potential therapeutic target such as asthma, multiple sclerosis, and many bleeding disorders (54, 55).

A mild response to the introduction of siRNA-LNPs was observed in the acute phase, but prolonged and repeated exposure was not associated with chronic systemic inflammation. The response appeared to be independent of plasminogen knockdown, but may have been induced by the siRNA component, since mild elevation of AST was observed after exposure to LNPs containing siRNA compared to empty LNPs. Toxicity to other tissues is not expected because previous studies have suggested that 90% of LNPs localize to the liver (38).

Improved LNP formulations that have decreased toxicity and enable the use of lower doses of siRNA are expected to alleviate this response. Dogs are sensitive to lipid nanoparticles, exhibiting a diverse set of reactions (56), this has limited their use as a model for investigating LNP-based therapies. Here, we show that after the first exposure to siRNA-LNPs, a 0.054 mg/kg dose enabled potent knockdown in dogs without severe toxicity or systemic inflammation; this dose is approximately 10-fold lower than the equivalent dose of the clinically approved siRNA-LNP drug, Onpatro, 0.3 mg/kg, converted using body surface area ratios from the FDA guidelines (36, 57).

A limitation of this work was the inclusion of only a single LNP formulation for the delivery of this siRNA. Although this MC3 formulation is the clinical standard for hepatic delivery, recent advances in the potency of LNP for RNA therapies would likely enable improved hepatotoxicity and inflammatory profiles. Furthermore, while the results in the canine model of HA were consistent with those in mice, the inter-animal variability in the canine model is relatively large (26), and this study was limited by a small sample size. Further exploration in a larger cohort of FVIII-deficient dogs or dogs with other bleeding disorders is required to validate a difference in annualized bleeding rate. An appropriately powered follow-up study. Although we foresee this being an effective strategy for bleeding disorders of various causes, this study was limited to only

testing the impact in models of FVIII deficiency. Future studies should consider the use of this strategy in the many indications where TXA is effective.

The efficacy of siPIg is similar to TXA, but lasts for weeks rather than hours after administration. TXA is effective for reducing blood loss in many scenarios, and in patients with increased risk of bleeding due to diverse etiologies, thus siPIg may be useful in the same scenarios if translated to humans. Although further study is needed, we envisage that this agent may be useful in other contexts of high fibrinolysis, such as in bleeding in mucosal tissues, or disorders such as α 2-antiplasmin deficiency, plasminogen activator inhibitor-1 deficiency, or Quebec platelet disorder (3, 58).

MATERIALS AND METHODS

Study design

The aim of this study was to develop a long-lasting antifibrinolytic, using LNP-delivered siRNA that targets plasminogen, and to evaluate the efficacy of this strategy to decrease bleeding in animal models of HA. First, plasminogen knockdown was assessed by measuring mRNA and protein in liver tissue and blood circulation, respectively. Once knockdown was established, markers of toxicity were evaluated, fibrinolysis was visualized in blood samples *ex vivo*, and bleeding tendency was compared with or without treatment in FVIII-deficient mice and dogs. Treatments were randomly assigned. Investigators were not blinded to treatment groups. Replicates varied depending on the experiment according to standard deviation and power analysis. Quantification of plasminogen was done in technical triplicate in mice ($n = 3$ per timepoint) and dogs [$n = 1$ (0.54 mg/kg), 2 (0.054 mg/kg), or 3 (0.027 mg/kg)]. After long-term repeat dosing of siRNA-LNPs in mice, periodontal bone loss was measured at six predetermined sites ($n = 6-7$), body weight, inflammatory markers, and fibrin deposition were also assessed ($n = 6-10$). Analysis of acute hepatotoxicity and inflammation 4 hours after administration of siRNA-LNPs was done in wild type C57BL/6 mice ($n = 5$). Bleeding challenges were performed in WT and FVIII-deficient mice using saphenous vein puncture ($n = 5-7$) and tail vein transection ($n = 7-10$) models. Fibrinolysis and impacts on spontaneous bleeding were evaluated in dogs of Irish setter background with FVIII deficiency ($n = 2$).

siRNA-LNP preparation

2'O-methylated siRNA against murine plasminogen (sense: GCAAACCUCUGCUUACUAAAGCUT, antisense: AAGCUUUAGUAAGCAGAGGUUUUGCUC) and canine plasminogen (sense: AAGCAAGAACUUGAAGAUGAAUUAC, antisense: GUAAUUCAUCUUCAAGUUCUUGCUUGG), obtained commercially (Integrated DNA Technologies), was dissolved in 25 mM sodium acetate pH 4 buffer at an amine-to-phosphate (N/P) ratio of 3. Lipids DLin-MC3-DMA, distearoylphosphatidylcholine (DSPC), cholesterol and polyethylene glycol (PEG-DMG), were dissolved in ethanol at a molar ratio of 50/10/38.5/1.5 mol%, respectively, to achieve a final concentration of 20 mM total lipid. The two solutions were

mixed using a T-junction mixer as described previously (59). The resulting lipid nanoparticles were dialysed against 1000-fold v/v phosphate buffered saline (PBS) pH 7.4. Cholesterol content was measured using a Cholesterol E Assay Kit (Wako Chemicals), from which total lipid concentration was extrapolated. Nucleic acid entrapment was determined using a RiboGreen assay (60).

siRNA-LNP administration and subsequent blood draws

Animal studies were performed in accordance with the University of British Columbia, Queen's University, Medical College of Wisconsin, and University of North Carolina approved protocols. Mouse strains were of C57BL/6J, B6129SF2/J, and B6;129S-F8tm1Kaz/J (Jackson Labs, stock #000664, #101045, #004424). All studies in mice, except that reported in fig. S3, A and B, used a dose of 1 mg siRNA/kg body weight administered via tail vein or retro-orbital venous sinus injection. Blood samples used to assess plasma protein were collected via saphenous vein puncture into heparinized capillaries or via retro-orbital bleeds, no more frequently than once every two weeks. Blood was drawn for coagulation assays from isoflurane-anesthetized mice by cardiac puncture using a 23G needle containing sodium citrate (109 mM) to a final v/v concentration of 10% in whole blood. To collect plasma, whole blood spun at 800 x g for 10 minutes.

For dogs, siRNA-LNPs were diluted up to 20 mL in saline, and administered IV directly following administration of dexamethasone (IV, 5 mg/kg), diphenhydramine (IM, 1 mg/kg), and famotidine (IM, 0.5 mg/kg); dogs were also administered prednisone (PO, 5 mg/kg), diphenhydramine (PO, 2.2 mg/kg), and famotidine (PO, 0.5 mg/kg) each morning and evening prior to siRNA-LNP infusion. After testing three doses in wild-type dogs of hound background (0.54, 0.054, and 0.027 mg/kg), two hemophilia A dogs (ages 6 and 7, from an Irish Setter background) were administered siPIg at 0.054 mg/kg.

mRNA quantification

Livers were surgically removed from anesthetized mice and tissue was homogenized in Trizol (ThermoFisher, Waltham, MA). Nucleic acid was isolated after phenol-chloroform extraction. DNA was digested by incubating the sample with TURBO DNase (ThermoFisher Scientific) at 37°C for 1 hour. DNase was removed by repeating the Trizol-chloroform extraction. Reverse transcription was performed using the iScript cDNA Synthesis Kit (Bio-Rad) followed by qPCR with SYBR Green Master Mix (ThermoFisher Scientific) and DNA primers (Integrated DNA Technologies) against *Plg* (F: TTCTTGGGGTCTTGGCTGTG, R: AGAGGTTTTGCTCGGCCTTC) and *Ppia* (F: GCGTCTCCTTCGAGCTGTT, R: TGTAAGTCACCACCCTGGC) or Taqman probes (ThermoFisher Scientific) against *Plg*, *Tnfa*, *Adgre1*, and *Ii6*.

Western blotting

Samples were reduced, boiled, and separated on 4 – 15% acrylamide gradient gels (Bio-Rad). After electrophoresis, the samples were transferred to a nitrocellulose membrane (GE Healthcare) and blocked with Odyssey Blocking Buffer (LI-COR). The membranes were treated with a primary antibody against plasminogen (1:1000; SAPG-AP; confirmed cross-reactivity: human, rat, mouse, rabbit, canine, pig; Affinity Biologicals), washed, and treated with HRP-labeled anti-host secondary antibody (1:15,000; Abcam). Specific bands were imaged using Clarity ECL (Bio-Rad) on film (Mandel). Quantification of western blots was done using ImageJ (NIH) to measure band intensity relative to background and loading controls.

Histopathology

To measure periodontal bone loss in mice, samples were defleshed and stained with methylene blue, then the distance between the cemento-enamel junction and alveolar bone crest was measured at six predetermined sites as previously described (24).

To measure fibrin deposition, mouse liver and lung tissue samples were fixed in neutral buffered formalin solution (Sigma-Aldrich) immediately after sacrifice. Tissues were then embedded in paraffin, sectioned, and stained via standard procedure with hematoxylin and eosin stain and immune labelling against fibrinogen (anti-murine fibrinogen antibody, R-4025; made in-house).

To visualize fibrin structure within clots, whole blood was collected from treated mice, clotted *ex vivo* for two hours, then fixed, embedded, sectioned, and stained, as described above.

Plasma multiplex cytokine analysis

Ten proinflammatory biomarkers (IFN- γ , IL-1 β , IL-2, IL-4, IL-5, IL-6, IL-10, IL-12p70, KC/GRO, TNF- α) were measured in plasma collected from mice four hours after first administration of siRNA-LNPs, or after nine months of repeated dosing, using an electrochemiluminescence-based enzyme-linked immunosorbent assay (K15048D; Meso Scale Discovery).

Thromboelastography (TEG)

Shear elastic moduli were evaluated at 37°C using a TEG Hemostasis Analyzer System 5000 (Haemoscope Corp). Citrated mouse whole blood or canine plasma was combined with CaCl₂ (10 mM), thrombin (0.03 nM Innovin, MedCorp), and tissue plasminogen activator (tPA; 3.8 nM) over 3 h.

Murine bleeding models

Two weeks after siPIg administration, mice were anesthetized with 10-15% isoflurane. For saphenous vein puncture, mice were placed supine on a heating pad, and inner leg fur was removed. Saphenous vein was visualized under a 20x magnification stereoscope, and isolated from artery, nerve, and connective tissue. After an approximately 5-minute rest period, to negate the impact of any venous constriction during isolation, puncture wound was made using the bevel of a 28 gauge needle. Blood was absorbed into pre-weighed filter paper and blood loss was measured from net weight.

Assessment of bleeding after tail tip injuries were performed using tail vein transection as described previously (61). Bleeding was induced two weeks after siPIg administration, and blood loss was quantified by measurement of hemoglobin concentrations.

Mice were weighed before bleeding challenge.

Thrombin and plasmin generation assays

Thrombin generation was measured by calibrated automated thrombography similar to methods described previously (62). Briefly, 10 μ L bovine serum albumin (BSA, 5 mg/mL) buffer containing silica/phospholipids (1:300 (v/v) final concentration) or 10 μ L thrombin calibrator (α 2-macroglobulin-thrombin) was added to 40 μ L diluted canine plasma (1:2 dilution, 20 μ L plasma: 40 μ L HBS).

Plasmin generation was measured based on cleavage of a plasmin-specific fluorogenic substrate (63, 64). To trigger plasmin generation, 10 μ L BSA solution (5 mg/mL) containing silica/phospholipids and rtPA (Alteplase) or 10 μ L plasmin calibrator (α 2-macroglobulin-plasmin) were added to 40 μ L diluted canine plasma. Final concentrations were: silica/phospholipids (1:300 dilution), rtPA (0.31 μ g/mL), CaCl_2 (16.6 mmol/L) and fluorogenic substrate (0.5 mmol/L Boc-Glu-Lys-Lys-AMC).

Reactions were initiated by adding 10 μ L substrate/calcium solution and monitored every 20 seconds with a fluorometer (Fluoroskan Ascent, Thrombinoscope) equipped with a 390/460 filter set (excitation/emission) for 2 hours (65).

Statistical analysis

Statistical analyses were performed using GraphPad Prism 8.0.1. All results presented in graphs are the mean \pm SEM. N indicates number of biological replicates. Two-tailed unpaired Student's t test was used to compare two data sets. Two-way analysis of variance (ANOVA) was used to compare two data sets over time, one-way ANOVA was used to compare multiple data sets with one variable. Welch's ANOVA was used when variance was not equal (Brown-Forsythe), all data was of normal distribution (Shapiro-Wilk). Significance was designated at P values < 0.05.

List of Supplementary Materials

Fig. S1 to S4.

Data file S1

References

1. M. Nesheim, Thrombin and fibrinolysis. *Chest* **124**, 33S–9S (2003).
2. G. Cesarman-Maus, K. A. Hajjar, Molecular mechanisms of fibrinolysis. *Br. J. Haematol.* **129**, 307–321 (2005).
3. J. C. Chapin, K. A. Hajjar, Fibrinolysis and the control of blood coagulation. *Blood Rev.* **29**, 17–24 (2015).
4. S. He, M. Blombäck, G. Jacobsson Ekman, U. Hedner, The role of recombinant factor VIIa (FVIIa) in fibrin structure in the absence of FVIII/FIX. *J. Thromb. Haemost.* **1**, 1215–1219 (2003).
5. K. E. Brummel-Ziedins, R. F. Branda, S. Butenas, K. G. Mann, Discordant fibrin formation in hemophilia. *J. Thromb. Haemost.* **7**, 825–832 (2009).
6. G. J. Broze, D. A. Higuchi, Coagulation-dependent inhibition of fibrinolysis: Role of carboxypeptidase-U and the premature lysis of clots from hemophilic plasma. *Blood* **88**, 3815–3823 (1996).
7. L. O. Mosnier, T. Lisman, H. M. van den Berg, H. K. Nieuwenhuis, J. C. Meijers, B. N. Bouma, The defective down regulation of fibrinolysis in haemophilia A can be restored by increasing the TAFI plasma concentration. *Thromb. Haemost.* **86**, 1035–1039 (2001).
8. M. J. Manco-Johnson, T. C. Abshire, A. D. Shapiro, B. Riske, M. R. Hacker, R. Kilcoyne, J. D. Ingram, M. L. Manco-Johnson, S. Funk, L. Jacobson, L. A. Valentino, W. K. Hoots, G. R. Buchanan, D. DiMichele, M. Recht, D. Brown, C. Leissinger, S. Bleak, A. Cohen, P. Mathew, A. Matsunaga, D. Medeiros, D. Nugent, G. A. Thomas, A. A. Thompson, K. McRedmond, J. M. Soucie, H. Austin, B. L. Evatt, Prophylaxis versus Episodic Treatment to Prevent Joint Disease in Boys with Severe Hemophilia. *N. Engl. J. Med.* **357**, 535–544 (2007).
9. I. M. Nilsson, Clinical pharmacology of aminocaproic and tranexamic acids. *J. Clin. Pathol. Suppl. (R. Coll. Pathol.)* **14**, 41–7 (1980).
10. L. J. Juang, W. S. Hur, L. M. Silva, A. W. Strilchuk, B. Francisco, J. Leung, M. K. Robertson, D. J. Groeneveld, B. La Prairie, E. M. Chun, A. P. Cap, J. P. Luyendyk, J. S. Palumbo, P. R. Cullis, T. H. Bugge, M. J. Flick, C. J. Kastrup, Suppression of fibrin(ogen)-driven pathologies in disease models through controlled knockdown by lipid nanoparticle delivery of siRNA. *Blood* **139**, 1302–1311 (2022).
11. H. R. Büller, C. Bethune, S. Bhanot, D. Gailani, B. P. Monia, G. E. Raskob, A. Segers, P. Verhamme, J. I. Weitz, FXI-ASO TKA Investigators, Factor XI antisense oligonucleotide for prevention of venous thrombosis. *N. Engl. J. Med.* **372**, 232–40 (2015).
12. A. S. Revenko, D. Gao, J. R. Crosby, G. Bhattacharjee, C. Zhao, C. May, D. Gailani, B. P. Monia, A. R. MacLeod, Selective depletion of plasma prekallikrein or coagulation factor XII inhibits thrombosis in mice without increased risk of bleeding. *Blood* **118**, 5302–11 (2011).
13. A. W. Strilchuk, S. C. Meixner, J. Leung, N. Safikhan, J. A. Kulkarni, H. M. Russell, R. van der Meel, M. R. Sutherland, A. P. Owens III, J. Palumbo, E. M. Conway, E. L. G. Pryzdial, P. Cullis, C. J. Kastrup, Sustained Depletion of FXIII-A by Inducing Acquired FXIII-B Deficiency. *Blood* (2020), doi:10.1182/blood.2020004976.
14. F. Ferrareso, A. W. Strilchuk, L. J. Juang, L. G. Poole, J. P. Luyendyk, C. J. Kastrup, Comparison of DLin-MC3-DMA and ALC-0315 for siRNA Delivery to Hepatocytes and Hepatic

Stellate Cells. *Mol. Pharm.* (2022), doi:10.1021/acs.molpharmaceut.2c00033.

15. A. Sehgal, S. Barros, L. Ivanciu, B. Cooley, J. Qin, T. Racie, J. Hettinger, M. Carioto, Y. Jiang, J. Brodsky, H. Prabhala, X. Zhang, H. Attarwala, R. Hutabarat, D. Foster, S. Milstein, K. Charisse, S. Kuchimanchi, M. A. Maier, L. Nechev, P. Kandasamy, A. V. Kel'In, J. K. Nair, K. G. Rajeev, M. Manoharan, R. Meyers, B. Sorensen, A. R. Simon, Y. Dargaud, C. Negrier, R. M. Camire, A. Akinc, An RNAi therapeutic targeting antithrombin to rebalance the coagulation system and promote hemostasis in hemophilia. *Nat. Med.* **21**, 492–497 (2015).
16. L. R. Baden, H. M. El Sahly, B. Essink, K. Kotloff, S. Frey, R. Novak, D. Diemert, S. A. Spector, N. Rouphael, C. B. Creech, J. McGettigan, S. Khetan, N. Segall, J. Solis, A. Brosz, C. Fierro, H. Schwartz, K. Neuzil, L. Corey, P. Gilbert, H. Janes, D. Follmann, M. Marovich, J. Mascola, L. Polakowski, J. Ledgerwood, B. S. Graham, H. Bennett, R. Pajon, C. Knightly, B. Leav, W. Deng, H. Zhou, S. Han, M. Ivarsson, J. Miller, T. Zaks, Efficacy and Safety of the mRNA-1273 SARS-CoV-2 Vaccine. *N. Engl. J. Med.* **384**, 403–416 (2020).
17. D. Adams, A. Gonzalez-Duarte, W. D. O'Riordan, C.-C. Yang, M. Ueda, A. V. Kristen, I. Tournev, H. H. Schmidt, T. Coelho, J. L. Berk, K.-P. Lin, G. Vita, S. Attarian, V. Planté-Bordeneuve, M. M. Mezei, J. M. Campistol, J. Buades, T. H. Brannagan, B. J. Kim, J. Oh, Y. Parman, Y. Sekijima, P. N. Hawkins, S. D. Solomon, M. Polydefkis, P. J. Dyck, P. J. Gandhi, S. Goyal, J. Chen, A. L. Strahs, S. V. Nochur, M. T. Sweetser, P. P. Garg, A. K. Vaishnav, J. A. Gollob, O. B. Suhr, Patisiran, an RNAi Therapeutic, for Hereditary Transthyretin Amyloidosis. *N. Engl. J. Med.* **379**, 11–21 (2018).
18. F. P. Polack, S. J. Thomas, N. Kitchin, J. Absalon, A. Gurtman, S. Lockhart, J. L. Perez, G. Pérez Marc, E. D. Moreira, C. Zerbini, R. Bailey, K. A. Swanson, S. Roychoudhury, K. Koury, P. Li, W. V Kalina, D. Cooper, R. W. Frenck, L. L. Hammitt, Ö. Türeci, H. Nell, A. Schaefer, S. Ünal, D. B. Tresnan, S. Mather, P. R. Dormitzer, U. Şahin, K. U. Jansen, W. C. Gruber, Safety and Efficacy of the BNT162b2 mRNA Covid-19 Vaccine. *N. Engl. J. Med.* **383**, 2603–2615 (2020).
19. R. Stagaard, C. D. Ley, K. Almholt, L. H. Olsen, T. Knudsen, M. J. Flick, Absence of functional compensation between coagulation factor VIII and plasminogen in double-knockout mice. *Blood Adv.* **2**, 3126–3136 (2018).
20. T. C. Nichols, C. Hough, H. Agersø, M. Ezban, D. Lillicrap, Canine models of inherited bleeding disorders in the development of coagulation assays, novel protein replacement and gene therapies. *J. Thromb. Haemost.* **14**, 894–905 (2016).
21. C. B. Keragala, R. L. Medcalf, Plasminogen: an enigmatic zymogen. *Blood* **137**, 2881–2889 (2021).
22. R. C. Tait, I. D. Walker, J. A. Conkie, S. I. Islam, F. McCall, R. Mitchell, J. F. Davidson, Plasminogen levels in healthy volunteers--influence of age, sex, smoking and oral contraceptives. *Thromb. Haemost.* **68**, 506–510 (1992).
23. T. H. Bugge, K. W. Kombrinck, M. J. Flick, C. C. Daugherty, M. J. Danton, J. L. Degen, Loss of fibrinogen rescues mice from the pleiotropic effects of plasminogen deficiency. *Cell* **87**, 709–719 (1996).
24. L. M. Silva, A. D. Doyle, T. Greenwell-Wild, N. Dutzan, C. L. Tran, L. Abusleme, L. J. Juang, J. Leung, E. M. Chun, A. G. Lum, C. S. Agler, C. E. Zuazo, M. Sibree, P. Jani, V. Kram, D. Martin, K. Moss, M. S. Lionakis, F. J. Castellino, C. J. Kastrup, M. J. Flick, K. Divaris, T. H. Bugge, N. M. Moutsopoulos, Fibrin is a critical regulator of neutrophil effector function at the oral

mucosal barrier. *Science* (80-.). **374**, eabl5450 (2021).

25. T. H. Bugge, M. J. Flick, C. C. Daugherty, J. L. Degen, Plasminogen deficiency causes severe thrombosis but is compatible with development and reproduction. *Genes Dev.* , 794–807 (1995).

26. G. N. Nguyen, J. K. Everett, S. Kafle, A. M. Roche, H. E. Raymond, J. Leiby, C. Wood, C.-A. Assenmacher, E. P. Merricks, C. T. Long, H. H. Kazazian, T. C. Nichols, F. D. Bushman, D. E. Sabatino, A long-term study of AAV gene therapy in dogs with hemophilia A identifies clonal expansions of transduced liver cells. *Nat. Biotechnol.* **39**, 47–55 (2021).

27. K. P. van Galen, E. T. Engelen, E. P. Mauser-Bunschoten, R. J. van Es, R. E. Schutgens, Antifibrinolytic therapy for preventing oral bleeding in patients with haemophilia or Von Willebrand disease undergoing minor oral surgery or dental extractions. *Cochrane database Syst. Rev.* **4**, CD011385 (2019).

28. R. Post, M. R. Germans, M. A. Tjerkstra, M. D. I. Vergouwen, K. Jellema, R. W. Koot, N. D. Kruijt, P. W. A. Willems, J. F. C. Wolfs, F. C. de Beer, H. Kieft, D. Nanda, B. van der Pol, G. Roks, F. de Beer, P. H. A. Halkes, L. J. A. Reichman, P. J. A. M. Brouwers, R. M. van den Berg-Vos, V. I. H. Kwa, T. C. van der Ree, I. Bronner, J. van de Vlekkert, H. P. Bienfait, H. D. Boogaarts, C. J. M. Klijn, R. van den Berg, B. A. Coert, J. Horn, C. B. L. M. Majoie, G. J. E. Rinkel, Y. B. W. E. M. Roos, W. P. Vandertop, D. Verbaan, R. Post, M. R. Germans, M. A. Tjerkstra, M. D. I. Vergouwen, K. Jellema, R. W. Koot, N. D. Kruijt, P. W. A. Willems, J. F. C. Wolfs, F. C. de Beer, H. Kieft, D. Nanda, B. van der Pol, G. Roks, F. de Beer, P. H. A. Halkes, L. J. A. Reichman, P. J. A. M. Brouwers, R. M. van den Berg-Vos, V. I. H. Kwa, T. C. van der Ree, I. Bronner, H. P. Bienfait, H. D. Boogaarts, C. J. M. Klijn, M. van Bilzen, H. J. G. Dieks, K. de Gans, J. B. M. ten Holter, J. R. de Kruijk, C. T. J. M. Leijzer, D. Molenaar, R. J. van Oostenbrugge, J. van Pamelan, F. H. M. Spaander, S. E. Vermeer, J. van de Vlekkert, J. M. Voorend, R. van den Berg, B. A. Coert, J. Horn, C. B. L. M. Majoie, G. J. E. Rinkel, Y. B. W. E. M. Roos, W. P. Vandertop, D. Verbaan, Ultra-early tranexamic acid after subarachnoid haemorrhage (ULTRA): a randomised controlled trial. *Lancet* **397**, 112–118 (2021).

29. C. C.-2 Trial, Effects of tranexamic acid on death, vascular occlusive events, and blood transfusion in trauma patients with significant haemorrhage (CRASH-2): a randomised, placebo-controlled trial. *Lancet* **376**, 23–32 (2010).

30. C. C.-3 Trial, Effects of tranexamic acid on death, disability, vascular occlusive events and other morbidities in patients with acute traumatic brain injury (CRASH-3): a randomised, placebo-controlled trial. *Lancet* **394**, 1713–1723 (2019).

31. P. S. Myles, J. A. Smith, A. Forbes, B. Silbert, M. Jayarajah, T. Painter, D. J. Cooper, S. Marasco, J. McNeil, J. S. Bussi eres, S. McGuinness, K. Byrne, M. T. V. Chan, G. Landoni, S. Wallace, Tranexamic Acid in Patients Undergoing Coronary-Artery Surgery. *N. Engl. J. Med.* **376**, 136–148 (2017).

32. A. Ockerman, T. Vanassche, M. Garip, C. Vandenbriele, M. M. Engelen, J. Martens, C. Politis, R. Jacobs, P. Verhamme, Tranexamic acid for the prevention and treatment of bleeding in surgery, trauma and bleeding disorders: a narrative review. *Thromb. J.* **19**, 54 (2021).

33. D. Wardrop, L. J. Estcourt, S. J. Brunskill, C. Doree, M. Trivella, S. Stanworth, M. F. Murphy, Antifibrinolytics (lysine analogues) for the prevention of bleeding in patients with haematological disorders. *Cochrane database Syst. Rev.* , CD009733 (2013).

34. A. Gayet-Ageron, D. Prieto-Merino, K. Ker, H. Shakur, F.-X. Ageron, I. Roberts, Effect of

treatment delay on the effectiveness and safety of antifibrinolytics in acute severe haemorrhage: a meta-analysis of individual patient-level data from 40 138 bleeding patients. *Lancet (London, England)* **391**, 125–132 (2018).

35. I. Roberts, H. Shakur, A. Afolabi, K. Brohi, T. Coats, Y. Dewan, S. Gando, G. Guyatt, B. J. Hunt, C. Morales, P. Perel, D. Prieto-Merino, T. Woolley, The importance of early treatment with tranexamic acid in bleeding trauma patients: an exploratory analysis of the CRASH-2 randomised controlled trial. *Lancet (London, England)* **377**, 1096–101, 1101.e1–2 (2011).

36. A. Akinc, M. A. Maier, M. Manoharan, K. Fitzgerald, M. Jayaraman, S. Barros, S. Ansell, X. Du, M. J. Hope, T. D. Madden, B. L. Mui, S. C. Semple, Y. K. Tam, M. Ciufolini, D. Witzigmann, J. A. Kulkarni, R. van der Meel, P. R. Cullis, The Onpattro story and the clinical translation of nanomedicines containing nucleic acid-based drugs. *Nat Nanotechnol* **14**, 1084–1087 (2019).

37. M. Jayaraman, S. M. Ansell, B. L. Mui, Y. K. Tam, J. Chen, X. Du, D. Butler, L. Eltepu, S. Matsuda, J. K. Narayanannair, K. G. Rajeev, I. M. Hafez, A. Akinc, M. A. Maier, M. A. Tracy, P. R. Cullis, T. D. Madden, M. Manoharan, M. J. Hope, Maximizing the Potency of siRNA Lipid Nanoparticles for Hepatic Gene Silencing In Vivo. *Angew. Chemie Int. Ed.* **51**, 8529–8533 (2012).

38. FDA, CENTER FOR DRUG EVALUATION AND MULTI-DISCIPLINE REVIEW Summary Review Office Director Clinical Statistical Clinical Pharmacology NDA (2018) (available at https://www.accessdata.fda.gov/drugsatfda_docs/nda/2018/210922Orig1s000MultiR.pdf).

39. J. L. Saes, S. E. M. Schols, K. F. Betbadal, M. van Geffen, K. Verbeek-Knobbe, S. Gupta, B. M. Hardesty, A. D. Shapiro, W. L. van Heerde, Thrombin and plasmin generation in patients with plasminogen or plasminogen activator inhibitor type 1 deficiency. *Haemophilia* **25**, 1073–1082 (2019).

40. C. Fenger-Eriksen, A. D. Lindholm, L. Krogh, T. Hell, M. Berger, M. Hermann, D. Fries, N. Juul, M. Rasmussen, A.-M. Hvas, Effect of Tranexamic Acid on Coagulation and Fibrin Clot Properties in Children Undergoing Craniofacial Surgery. *Thromb. Haemost.* **120**, 392–399 (2020).

41. R. Stagaard, M. J. Flick, B. Bojko, K. Goryński, P. Z. Goryńska, C. D. Ley, L. H. Olsen, T. Knudsen, Abrogating fibrinolysis does not improve bleeding or rFVIIa/rFVIII treatment in a non-mucosal venous injury model in haemophilic rodents. *J. Thromb. Haemost.* **16**, 1369–1382 (2018).

42. N. Vaezzadeh, R. Ni, P. Y. Kim, J. I. Weitz, P. L. Gross, Comparison of the effect of coagulation and platelet function impairments on various mouse bleeding models. *Thromb. Haemost.* **112**, 412–418 (2014).

43. A. E. Pastoft, J. Lykkesfeldt, M. Ezban, M. Tranholm, H. C. Whinna, B. Lauritzen, A sensitive venous bleeding model in haemophilia A mice: Effects of two recombinant FVIII products (N8 and Advate®). *Haemophilia* **18**, 782–788 (2012).

44. K. Tefs, M. Gueorguieva, J. Klammt, C. M. Allen, D. Aktas, F. Y. Anlar, S. D. Aydogdu, D. Brown, E. Ciftci, P. Contarini, C.-E. Dempfle, M. Dostalek, S. Eisert, A. Gökbuget, O. Günhan, A. A. Hidayat, B. Hügler, M. Isikoglu, M. Irkeç, S. K. Joss, S. Klebe, C. Kneppo, I. Kurtulus, R. P. Mehta, K. Ornek, R. Schneppenheim, S. Seregard, E. Sweeney, S. Turtschi, G. Veres, P. Zeitler, M. Ziegler, V. Schuster, Molecular and clinical spectrum of type I plasminogen deficiency: A series of 50 patients. *Blood* **108**, 3021–3026 (2006).

45. Y. Tashima, F. Banno, T. Kita, Y. Matsuda, H. Yanamoto, T. Miyata, Plasminogen Tochigi

- mice exhibit phenotypes similar to wild-type mice under experimental thrombotic conditions. *PLoS One* **12**, e0180981 (2017).
46. T. Celkan, Plasminogen deficiency. *J. Thromb. Thrombolysis* **43**, 132–138 (2017).
47. L. Martin-Fernandez, P. Marco, I. Corrales, R. Pérez, L. Ramírez, S. López, F. Vidal, J. M. Soria, The Unravelling of the Genetic Architecture of Plasminogen Deficiency and its Relation to Thrombotic Disease. *Sci. Rep.* **6**, 39255 (2016).
48. V. Schuster, B. Hügler, K. Tefs, Plasminogen deficiency. *J. Thromb. Haemost.* **5**, 2315–2322 (2007).
49. A. F. Drew, A. H. Kaufman, K. W. Kombrinck, M. J. Danton, C. C. Daugherty, J. L. Degen, T. H. Bugge, Ligneous conjunctivitis in plasminogen-deficient mice. *Blood* **91**, 1616–1624 (1998).
50. B. J. A., B. T. H., M.-A. Hector, S. Gregg, K. K. W., W. D. P., D. J. L., Plasminogen deficiency leads to impaired remodeling after a toxic injury to the liver. *Proc. Natl. Acad. Sci.* **96**, 15143–15148 (1999).
51. L. M. Silva, A. G. Lum, C. Tran, M. W. Shaw, Z. Gao, M. J. Flick, N. M. Moutsopoulos, T. H. Bugge, E. S. Mullins, Plasmin-mediated fibrinolysis enables macrophage migration in a murine model of inflammation. *Blood* **134**, 291–303 (2019).
52. K. Kolev, C. Longstaff, Bleeding related to disturbed fibrinolysis. *Br. J. Haematol.* **175**, 12–23 (2016).
53. Y. Song, N. Izumi, L. B. Potts, A. Yoshida, Tranexamic acid-induced ligneous conjunctivitis with renal failure showed reversible hypoplasminogenaemia. *BMJ Case Rep.* **2014**, bcr2014204138 (2014).
54. C. M. Swaisgood, M. A. Aronica, S. Swaidani, E. F. Plow, Plasminogen is an important regulator in the pathogenesis of a murine model of asthma. *Am. J. Respir. Crit. Care Med.* **176**, 333–342 (2007).
55. M. A. Shaw, Z. Gao, K. E. McElhinney, S. Thornton, M. J. Flick, A. Lane, J. L. Degen, J. K. Ryu, K. Akassoglou, E. S. Mullins, Plasminogen Deficiency Delays the Onset and Protects from Demyelination and Paralysis in Autoimmune Neuroinflammatory Disease. *J. Neurosci. Off. J. Soc. Neurosci.* **37**, 3776–3788 (2017).
56. J. Szebeni, C. R. Alving, L. Rosivall, R. Bünger, L. Baranyi, P. Bedöcs, M. Tóth, Y. Barenholz, Animal Models of Complement-Mediated Hypersensitivity Reactions to Liposomes and Other Lipid-Based Nanoparticles. *J. Liposome Res.* **17**, 107–117 (2007).
57. Food and Drug Administration, *Guidance for Industry: Estimating the Maximum Safe Starting Dose in Initial Clinical Trials for Therapeutics in Adult Healthy Volunteers* (2005).
58. J. Blavignac, N. Bunimov, G. E. Rivard, C. P. M. Hayward, Quebec platelet disorder: update on pathogenesis, diagnosis, and treatment. *Semin. Thromb. Hemost.* **37**, 713–720 (2011).
59. J. A. Kulkarni, M. M. Darjuan, J. E. Mercer, S. Chen, R. Van Der Meel, J. L. Thewalt, Y. Y. C. Tam, P. R. Cullis, On the Formation and Morphology of Lipid Nanoparticles Containing Ionizable Cationic Lipids and siRNA. *ACS Nano* **12**, 4787–4795 (2018).
60. S. Chen, Y. Y. C. Tam, P. J. C. Lin, M. M. H. Sung, Y. K. Tam, P. R. Cullis, Influence of particle size on the in vivo potency of lipid nanoparticle formulations of siRNA. *J. Control. Release* **235**, 236–244 (2016).

61. P. B. Johansen, M. Tranholm, J. Haaning, T. Knudsen, Development of a tail vein transection bleeding model in fully anaesthetized haemophilia A mice - characterization of two novel FVIII molecules. *Haemophilia* **22**, 625–631 (2016).
62. D. E. Madsen, T. C. Nichols, E. P. Merricks, E. K. Waters, B. Wiinberg, Global measurement of coagulation in plasma from normal and haemophilia dogs using a novel modified thrombin generation test - Demonstrated in vitro and ex vivo. *PLoS One* **12**, e0175030 (2017).
63. A. Miszta, A. K. Kopec, A. Pant, L. A. Holle, J. R. Byrnes, D. A. Lawrence, K. C. Hansen, M. J. Flick, J. P. Luyendyk, B. de Laat, A. S. Wolberg, A high-fat diet delays plasmin generation in a thrombomodulin-dependent manner in mice. *Blood* **135**, 1704–1717 (2020).
64. A. Miszta, H. K. Ahmadzia, N. L. C. Luban, S. Li, D. Guo, L. A. Holle, J. S. Berger, A. H. James, J. V. S. Gobburu, J. van den Anker, B. de Laat, A. S. Wolberg, Application of a plasmin generation assay to define pharmacodynamic effects of tranexamic acid in women undergoing cesarean delivery. *J. Thromb. Haemost.* **19**, 221–232 (2021).
65. H. C. Hemker, R. Kremers, Data management in thrombin generation. *Thromb. Res.* **131**, 3–11 (2013).

Acknowledgements

Funding

This work was supported by the Canadian Institutes of Health Research (CIHR) (FDN-148370, MSH-130166 to CJK), the Natural Sciences and Engineering Research Council (NSERC) (RGPIN 2018-04918 to CJK), the Canadian Foundation for Innovation (31928 to CJK), the BC Knowledge Development Fund (to CJK), and the Nanomedicines Innovation Network of the Networks of Centres of Excellence (NMIN) (to CJK); N Dos Santos and M Bally of the NMIN PharmaCore also provided technical assistance. This work was also supported by the National Institutes of Health (R01HL166382 to CJK, R01HL126974 to ASW, N0175N92019D00041 to TCN, R01HL102035 to QS), and the National Institute of Dental and Craniofacial Research (1K99DE030124-01A1 to LMS and THB); the content is solely the responsibility of the authors and does not necessarily represent the official views of the National Institutes of Health.

Author contributions

AWS designed and performed most experiments, analysis and interpretation of data, and writing of the paper. WSH, PB, YS, SRA, ASMY, JL, LMS, JAS, and KN helped design and perform experiments and edited the paper. BdL, NMM, THB, QS, PRC, EPM, ASW, MJF, DL, and TCN helped design experiments, interpret results, and edited the paper. CJK designed experiments, analyzed and interpreted data and edited the paper.

Competing interests

AWS, PRC, and CJK are directors and shareholders of SeraGene Therapeutics Inc., which is developing RNA-based therapies. PRC and CJK are directors and shareholders of NanoVation Therapeutics, Inc., which is developing lipid-based delivery platforms. PRC has financial interests in Acuitas Therapeutics and Mesentech. CJK has financial interests in CoMotion Drug Delivery Systems, and has consulted for Alnylam Pharmaceuticals. AWS, JL, PRC, and CJK have filed intellectual property on RNA-based therapies with the intention of commercializing these inventions, including “PCT/CA2022/050213: Methods and compositions for modulating plasminogen”. BdL is employed by Synapse Research Institute, a group that produces materials for thrombin and plasmin generation measurements in plasma. The other authors declare no competing interests.

Data and materials availability

All data associated with this study are present in the paper or the Supplementary Materials. siRNA-LNPs described in this work are available under a materials transfer agreement with the

University of British Columbia and Versiti Blood Research Institute; please contact ckastrup@versiti.org.

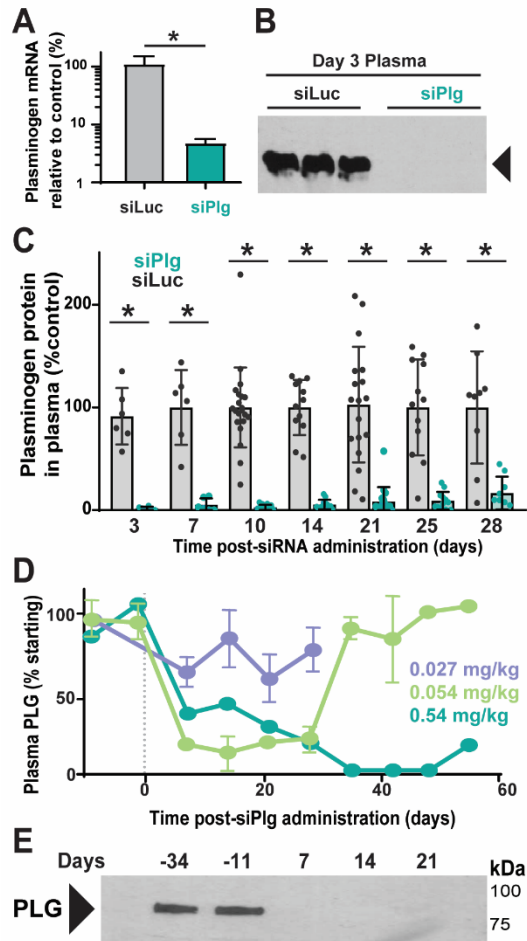


Figure 1: Plasminogen is depleted for weeks after a single administration of siPIg in mice and dogs. A) Mice were injected with a single dose of siLuc (grey) or siPIg (teal blue). *Plg* mRNA in liver tissue was measured using qPCR, normalized against the housekeeping gene, *Ppia*. **B)** Representative western blot against plasminogen, where each lane contains the plasma from an individual mouse in either treatment group. The triangular marker indicates the expected molecular weight of plasminogen (92 kDa). **C)** Plasminogen protein in plasma measured in a portion of the mice enrolled at each timepoint using densitometry, normalized to a loading control, and graphed relative to untreated mice. **D)** Plasminogen protein in plasma quantified after administration of siPIg to dogs at 0.027 (purple, $n = 3$), 0.054 (green, $n = 2$), or 0.54 (teal blue, $n = 1$) mg siRNA per kg body weight. **E)** Representative western blot against plasminogen, where each lane contains plasma collected from a single wild-type dog at a different timepoint before or after siPIg administration at 0.054 mg/kg. Data are presented as mean \pm SEM and were analyzed by two-tailed unpaired Student's t test (A) or by two-way ANOVA (C); * $P < 0.05$.

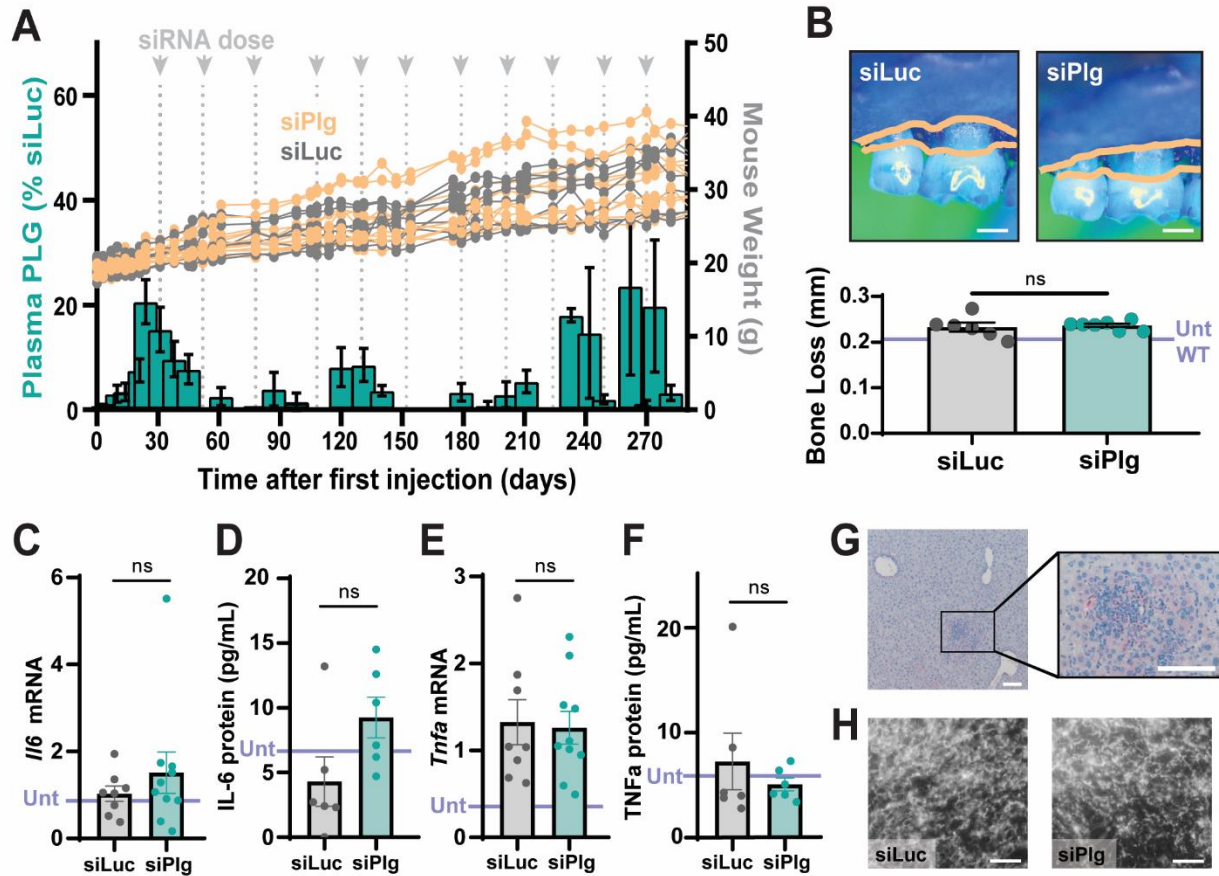


Figure 2: Long-term knockdown of plasminogen does not lead to pathologies associated with complete plasminogen deficiency. **A)** Plasma plasminogen (left Y axis) quantified during nine months of repeat administration of siPlg. The weight of mice (right Y axis) was tracked over this period during administration of siLuc (grey) and siPlg (orange). **B)** Periodontal bone loss measured by the distance between the cemento-enamel junction and the alveolar bone crest (orange lines; scale bar is 2 mm) in samples stained with methylene blue from mice administered siLuc ($n = 6$) or siPlg ($n = 7$) for nine months, compared to untreated (Unt WT) age-matched wild-type controls (purple line). **C to F)** Inflammatory markers IL-6 (C and D), and TNF- α (E and F) were measured using qPCR in liver tissue, or ELISA in plasma from siLuc ($n = 8$) or siPlg ($n = 10$) treated mice, compared to untreated (Unt) controls (purple line). **G)** Immunohistochemistry against fibrin(ogen) in microscopy images of liver tissue of siPlg-treated mice showed inflammatory infiltrates but no fibrinous lesions (scale bar is 100 μ m). **H)** Immunohistochemistry against fibrin(ogen) in clots formed ex vivo in whole blood from mice treated with siLuc (left) or siPlg (right) (scale bar is 25 μ m). For all graphs, values represent mean \pm SEM, ns indicates difference not statistically significant ($P > 0.05$), analyzed by two-tailed unpaired Student's t test.

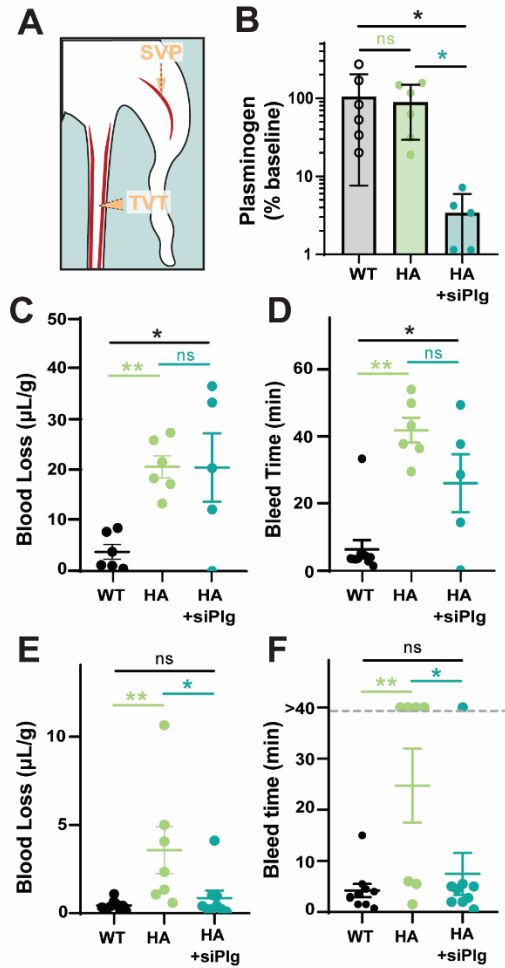


Figure 3: Plasminogen knockdown enhances hemostasis after saphenous vein puncture but not tail vein transection in a mouse model of hemophilia A. **A)** Schematic showing saphenous vein puncture (SVP) and tail vein transection (TVT) injury models. **B)** Plasminogen in HA mice at time of TVT bleed. **C and D)** Blood loss in μL blood per g body weight (C) and bleeding time (D) after TVT in WT, untreated HA, and treated HA mice ($n = 5-7$). **E and F)** Blood loss in μL blood per g body weight (E) and bleeding time (F) to end of observation period at 40 minutes (grey dashed line) after SVP ($n = 7-10$). Values represent mean \pm SEM; * $P < 0.05$, ** $P < 0.01$, and ns indicates not significant ($P > 0.05$), analyzed by one-way ANOVA.

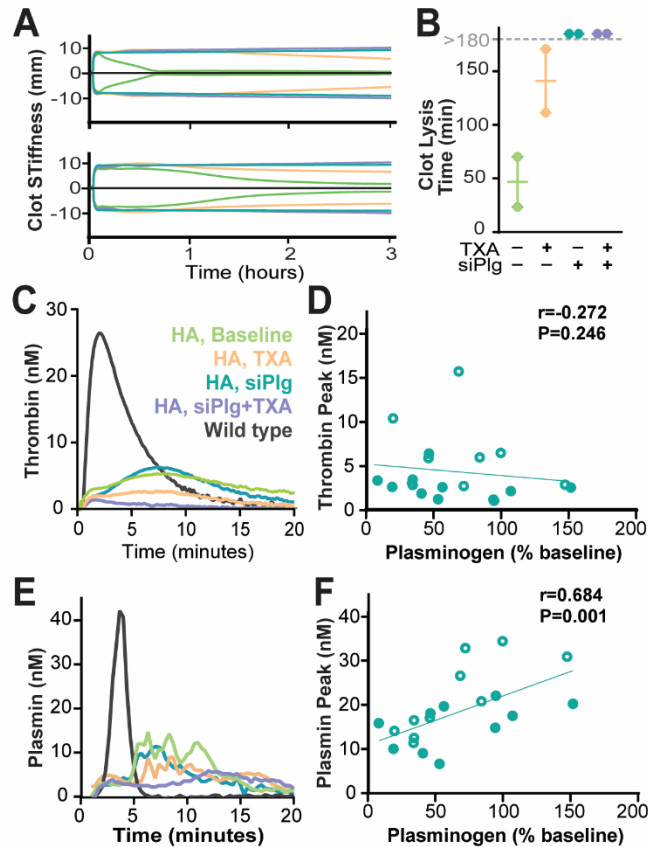


Figure 4: Plasminogen knockdown stabilizes clots ex vivo in two dogs with hemophilia A. Samples were collected from two HA dogs at baseline (green), within four hours of IV 10 mg/kg TXA (orange), within three weeks of siPIg administration without TXA (teal), or following administration of both siPIg and TXA (purple). **A)** Representative TEG curve tracings using plasma from two HA dogs (top and bottom graphs) with added tPA. **B)** Clot lysis time within 180-minute monitoring period, values represent mean, error bars represent \pm SEM. **C)** Thrombin generation in plasma collected weekly from two HA dogs, or pooled plasma from wild-type dogs (WT, grey). **D)** Correlation between plasminogen protein in plasma and thrombin generation peak (open and closed markers distinguish the two siPIg-treated dogs). **E)** Plasmin generation in plasma collected weekly from two HA dogs, or pooled plasma from WT dogs. **F)** Correlation between plasma plasminogen and plasmin generation peak.

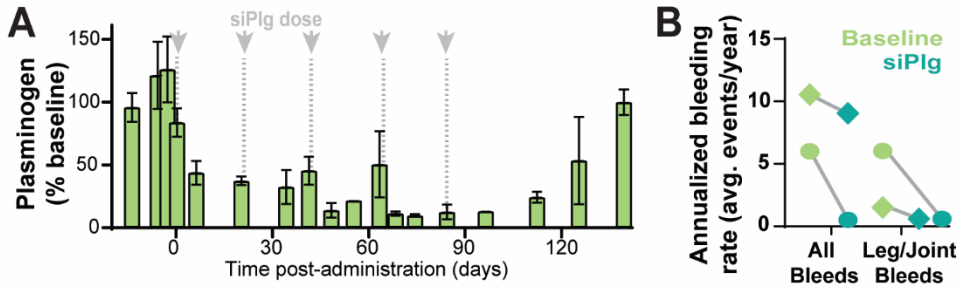


Figure 5: Plasminogen knockdown decreases bleeding events in two dogs with hemophilia A over a 4-month period. HA dogs were administered 5 doses of siPIg over 15 weeks. Vertical dashed lines indicate days of an administration. **A)** Plasminogen in plasma quantified using densitometry of western blots. Values represent mean \pm SEM. **B)** Annualized bleeding rate extrapolated from 10 months prior to treatment, and the 4-month period of siPIg treatment in two HA dogs (circle and diamond each indicate an individual dog).

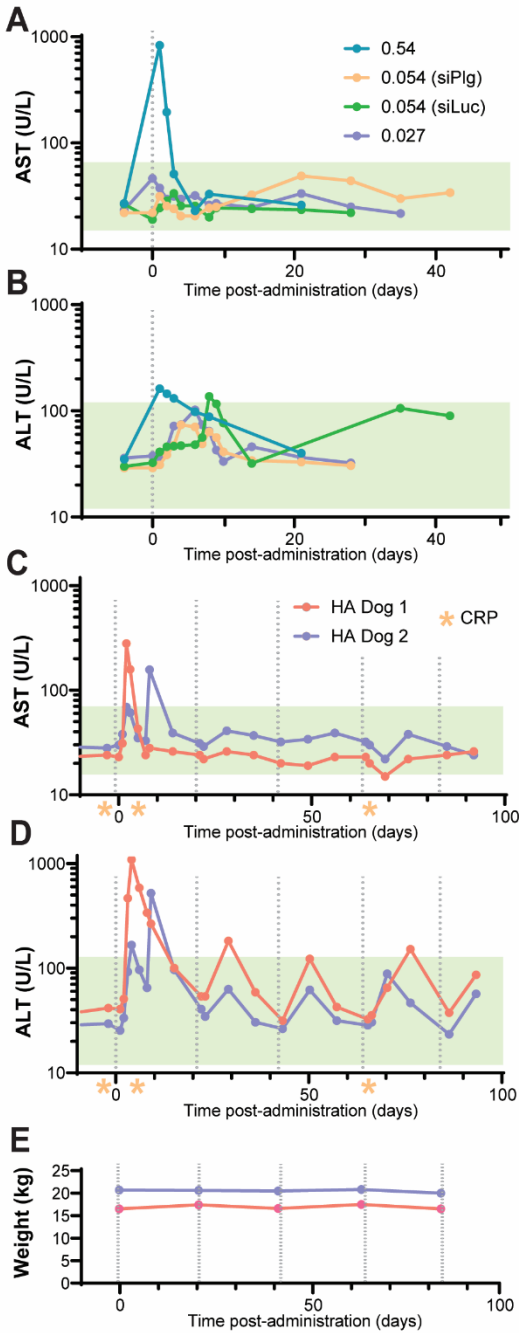


Figure S1: Hepatic sensitivity to injections of siRNA-LNPs is dose dependent, and not related to plasminogen knockdown. Markers of hepatotoxicity measured after administration of LNPs (vertical dashed lines indicate days of administration) carrying siPIg or siLuc; normal range is marked by the green box. **A and B)** Aspartate transaminase (AST, A) and alanine transaminase (ALT, B) after administration of siPIg at 0.54 mg/kg (blue), 0.054 mg/kg (orange), and 0.027 mg/kg (purple), or siLuc at 0.054 mg/kg (green) to WT dogs. **C and D)** Aspartate transaminase (AST, C) and alanine transaminase (ALT, D) after repeat administration of siPIg at 0.054 mg/kg to two hemophilia A dogs (purple and red). Yellow asterisk indicates timepoints at which CRP was measured. **E)** Weight of hemophilia A dogs during study.

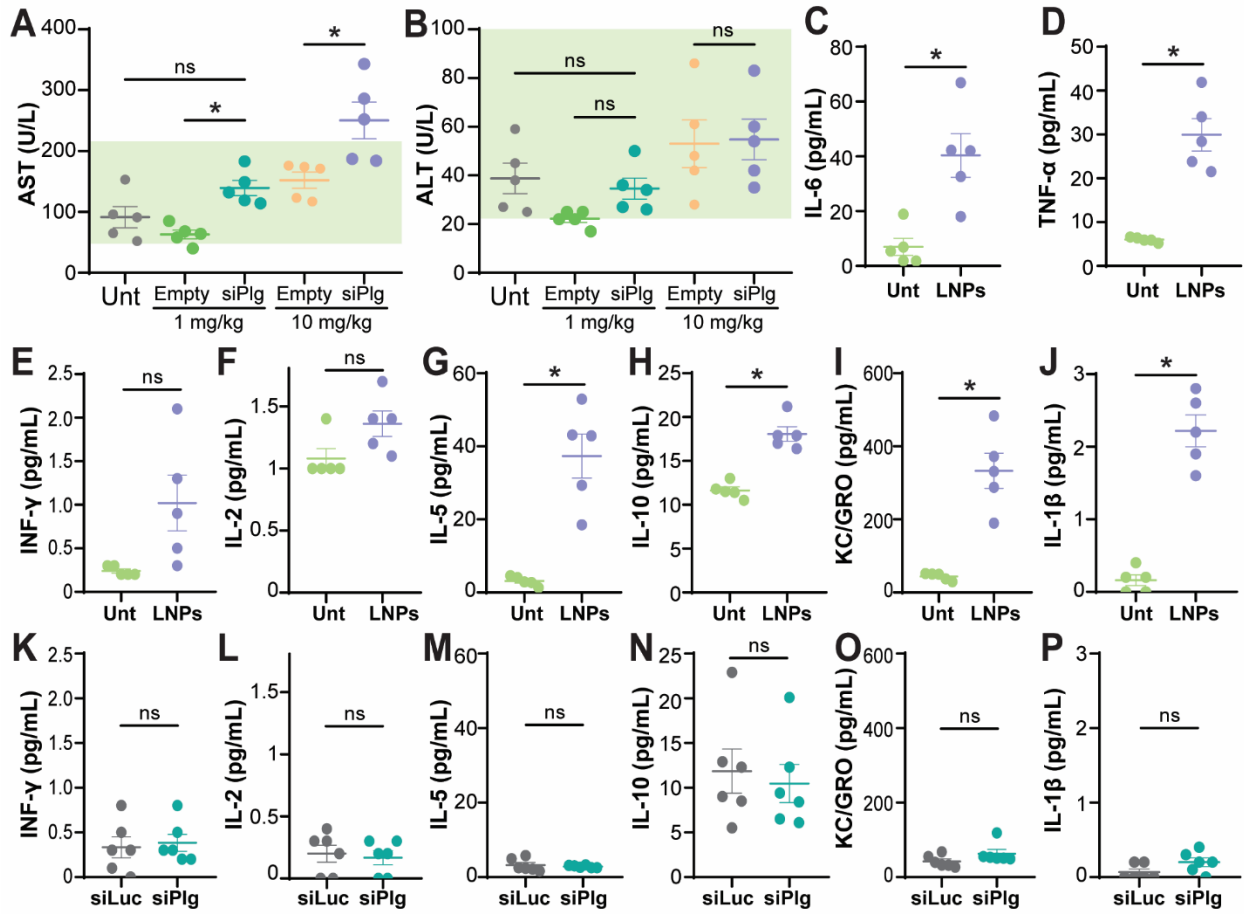


Figure S2: siRNA-LNPs cause an acute response but no long-term systemic inflammation in mice. A and B) AST and ALT were measured in plasma 4 hours after administration of empty LNPs or LNPs containing siRNA, at an effective dose (1 mg/kg) and a high dose (10 mg/kg) ($n = 5$); normal range is marked by the green box. **C to P)** Inflammatory markers were measured in plasma 4 hours after administration of siPIg (C to J, $n = 5$) or after 9 months of repeat administration of siLuc or siPIg (K to P, $n = 6$).

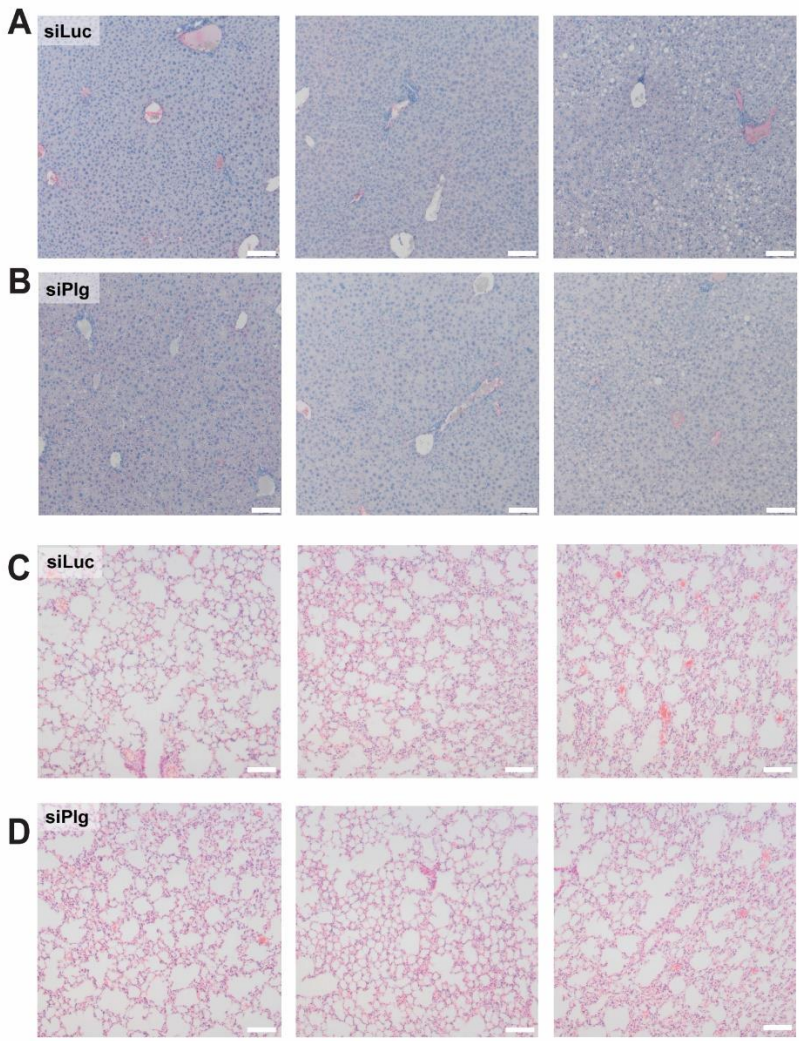


Figure S3: No apparent fibrin deposition in liver or lung tissue after prolonged plasminogen knockdown. A and B) Immunohistochemistry against fibrin(ogen) in microscopy images of liver tissue of mice treated with siLuc (A) or siPIg (B) for nine months. C and D) H&E stained sections of lung tissue from mice treated with siLuc (C) or siPIg (D) for 5 months. Scale bars, 100µm.

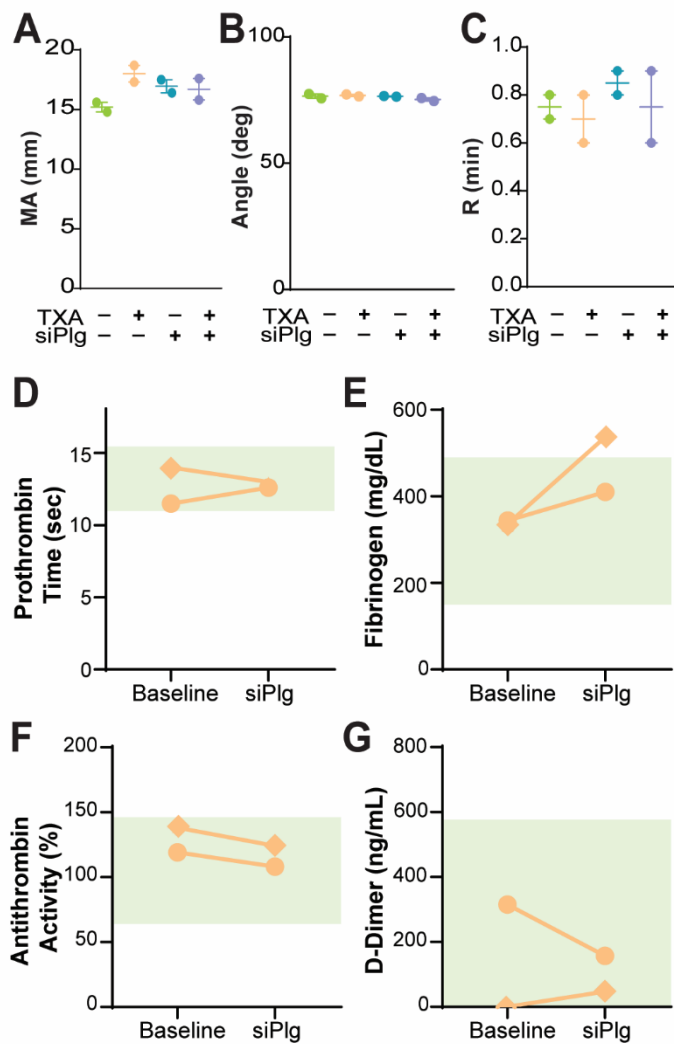


Figure S4: Indicators of thrombotic risk remain within normal range in HA dogs treated with siPIg. **A to C)** Maximum amplitude (A), alpha angle (B), and R-time (C) measured by thromboelastography of plasma collected from two HA dogs at baseline (green), within four hours of IV 10 mg/kg TXA (orange), within three weeks of siPIg administration without TXA (teal), or following administration of both siPIg and TXA (purple). **D to G)** Prothrombin time (D), clottable fibrinogen concentration (E), antithrombin activity (F), and D-dimer concentrations (G) were measured in plasma from two HA dogs before treatment, and after the 0.054 mg/kg dose of siPIg. Each line represents one dog at two timepoints, green shading indicates reference interval.